

Exciton annihilation in a polyfluorene: Low threshold for singlet-singlet annihilation and the absence of singlet-triplet annihilation

S. M. King, D. Dai, C. Rothe, and A. P. Monkman

Department of Physics, Durham University, South Road, Durham DH1 1LE, United Kingdom

(Received 1 May 2007; published 9 August 2007)

Ultrafast photoinduced absorption measurements have been used to directly investigate singlet-singlet annihilation in polyfluorene. The pump fluence threshold for annihilation to dominate the decay was measured to be $\sim 1 \mu\text{J cm}^{-2}$ corresponding to an excitation density of $1.5 \times 10^{17} \text{ cm}^{-3}$. The annihilation rate was found to be faster than that expected from a simple dipole-dipole interaction. This is ascribed to the additional influence of diffusion which, because of the dispersive nature of the exciton migration, has strong time dependence as the singlet excitons thermalize in the density of states as well as the expected intrinsic time dependence from a diffusion controlled process. Also, a comparable background level of triplets was created in the film to study the effect of singlet-triplet annihilation, which surprisingly, given the low threshold for singlet-singlet annihilation, was found to be negligible.

DOI: [10.1103/PhysRevB.76.085204](https://doi.org/10.1103/PhysRevB.76.085204)

PACS number(s): 78.66.Qn, 72.80.Le, 78.47.+p

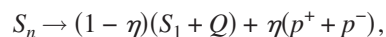
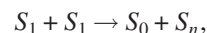
INTRODUCTION

Ever since the first reports of electroluminescence from conjugated polymers, the nature and dynamics of excitons in conjugated polymers have become of great importance to the scientific community.^{1,2} Especially important, with respect to the use of conjugated polymers for lighting and display applications, are the dynamics in the solid state and with the potential for high brightness devices and polymer lasers, the behavior of excitons at high excitation densities is becoming of interest.³⁻⁵ Most relevant are the mechanisms that can quench the excitons and represent a channel for the loss of efficiency of light emission.^{6,7} The blue emitting polyfluorenes are currently the most important class of conjugated polymers (CPs) for light emitting devices as they are able to produce high energy emission with a reasonable efficiency; the polymer poly-9,9-diethylhexylfluorene (PF2/6) is a well understood prototypical polyfluorene.⁸

Previous ultrafast studies have been made on conjugated polymers at varying excitation densities.⁹⁻¹¹ In most cases, fast components to the decay are observed. These fast components are due to fluorescence quenching, which causes a reduction in efficiency of the light emission. However, most previous experiments have been made at considerably greater excitation densities than this study. In many cases, photon fluences are as much as 2 orders higher than those used here. The nature of charge generation from singlet excitons is one such process that has been primarily studied at such high excitation densities. The result of this is that the data become complicated by the simultaneous observation of many processes and often small differences in the experimental conditions can change the dominance of the various processes, and therefore conclusions obtained can appear inconsistent.¹²⁻¹⁶ In many cases, the intensity dependent phenomena observed are present at the lowest excitation densities measured and as a result it can be difficult to reconcile with data from experiments such as time resolved fluorescence measurements which only require very low pump fluence.^{11,17} The result is that time resolved measurements on conjugated polymers often fall into two categories, high

pump dose and low pump dose with little data available in the crossover. This study is based around excitation density dependent measurements in this crucial area, showing the transition from the intrinsic phenomena to those at high excitation densities.

Two such intensity dependent processes which represent a loss of efficiency in conjugated polymer devices are the bimolecular singlet-singlet and singlet-triplet annihilation reactions.^{18,19} In these cases, excitation energy is transferred from an excited singlet to another excited singlet or triplet state. Singlet-singlet annihilation only occurs when the singlet excitation density becomes large enough that the singlets are able to interact with each other within their lifetime. Generally, it can be considered that such exciton annihilation reactions generate a highly excited singlet state which may rapidly return to the excited singlet state.²⁰ Alternatively, as the energy is sufficient to overcome the $\sim 0.4 \text{ eV}$ exciton binding energy, the exciton is able to dissociate into charges.^{21,22} The two possible are shown below.



where S_0 is the singlet ground state, S_1 is the excited singlet state, S_n represents higher excited singlet states which rapidly thermalize to S_1 with the release of heat (Q), and p^+ and p^- are a pair of charges which are generated with a proportion η

The case of singlet-triplet annihilation is especially relevant to the polymer light emitting diode (PLED) community due to the higher proportion of triplets formed in devices in comparison with photoexcitation. Additionally, their longer lifetime compared to singlets allows a large triplet population to build up during device operation. Considering this, if the rate of singlet-triplet quenching is significant, then it represents a major loss channel for singlet emission in devices.

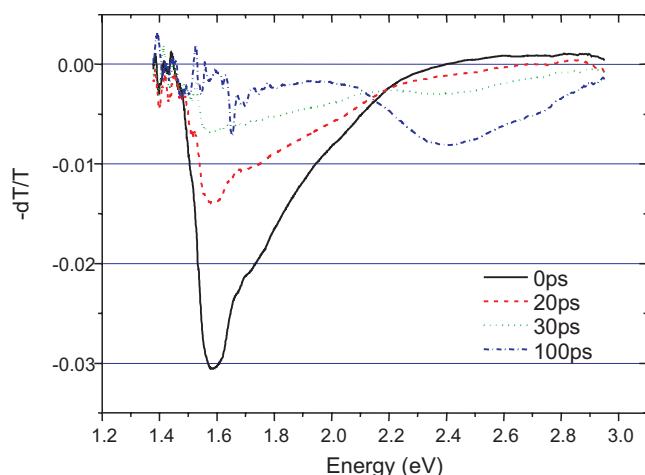


FIG. 1. (Color online) Time resolved photoinduced absorption spectra of a thin film of PF2/6 at various times after photoexcitation measured for an excitation density of $20 \mu\text{J cm}^{-2}$.

EXPERIMENT

Ultrafast photoinduced absorption (PA) measurements were made using a conventional femtosecond pump probe system. The system is based around a Coherent Mira 900-f femtosecond oscillator and RegA 9000 laser amplifier. The 180 fs, $\sim 4 \mu\text{J}$, 100 kHz pulses at 1.6 eV are split inside an OPA; 75% of the power is used to generate the 3.2 eV pump beam. The remaining portion is focused into a sapphire plate to generate a white light supercontinuum, which is either used directly as probe beam for measuring transient spectra with a diode array spectrometer or to seed the OPA and generate a single wavelength beam for measuring kinetics. This high repetition rate system is ideal for low pump fluence measurements, allowing high signal to noise ratios for low pump dose; overall, this allows the measurement of dT/T as small as 10^{-6} using lock-in detection.

Measurements to determine the extent of singlet-triplet annihilation were carried out using the same pump probe system. In addition, a background level of triplets was generated by a 50 mW, 3.06 eV diode laser, focused to a 0.5 cm^2 spot. At low temperature, the long lifetime of triplets in comparison with singlets allows a high background triplet population to be built up under cw excitation by the diode laser. The triplets appear as static quenching sites for the singlets because the singlets are comparatively mobile with respect to the triplet population.

Thin films of the pure polymer PF2/6 were spin cast from a toluene solution, yielding films of about 100 nm thick; all polymer handling was done in UV-light-free clean room to minimize the effects of sample degradation. Additionally, all experiments were carried out under dynamic vacuum of $\sim 10^{-5}$ mbar.

SINGLET-SINGLET ANNIHILATION

The transient absorption spectra of PF2/6 in Fig. 1 show similar features to those previously obtained for other conjugated polymers.^{9,23} Within our energy range, three main fea-

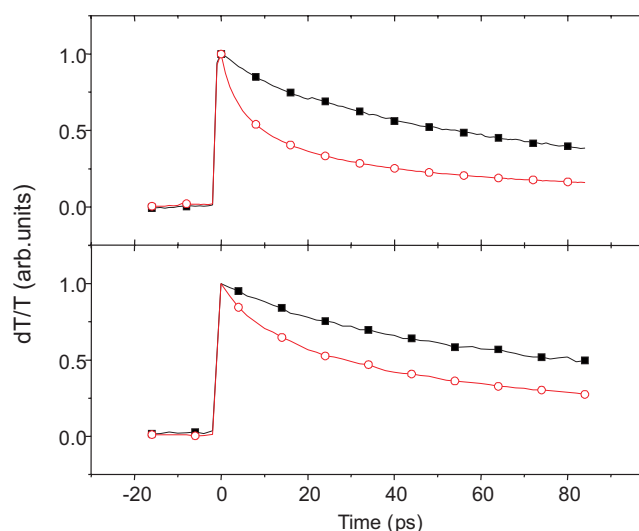


FIG. 2. (Color online) Decay of the PA singlet exciton feature (1.60 eV) for excitation dose of $25 \mu\text{J cm}^{-2}$ (○) and $7 \mu\text{J cm}^{-2}$ (■) at 300 K (top panel) and 10 K (bottom panel).

tures are observed. In the period immediately following excitation, a sharp absorption peak around 1.6 eV dominates; also immediately observed is a small amount of stimulated emission in the region of the photoluminescence at 2.8 eV. Many previous works on conjugated polymers have correlated the kinetics of these two features, unambiguously assigning the absorption at 1.6 eV to the S_1-S_n transition.^{11,23,24} At longer times, the spectral features due to the singlet exciton decay and are replaced by a broad absorption peak at 2.4 eV. Assignment of this feature as a charged state has been made before in field assisted pump probe experiments, where free carriers are generated and a similar absorption is observed.¹³ Pulse radiolysis and doping induced absorption studies also provide strong evidence that this feature is the absorption of the polyfluorene cation.²⁵ The clear isobestic point at 2.15 eV is a strong evidence that the charged state is formed as a direct result of the decay of the singlet exciton: it is a quenching product of the singlet exciton. The lack of absorption in this region immediately after photoexcitation is a direct proof that the charge carriers are not generated directly by optical absorption in this case.

The decay of the singlet transition at 1.6 eV is shown in Fig. 2; at low excitation dose ($0.35 \mu\text{J cm}^{-2}$), the unquenched lifetime is approximately 250 ps, similar to fluorescence lifetimes measured by time correlated single photon counting.²⁶ At high excitation densities, an additional fast component begins to dominate the decay. It is possible to quantify the change in the decay rate with excitation densities by comparing the intensity of the photoinduced absorption after 100 ps with the initial intensity of the absorption; this is shown in Fig. 3. It is apparent that the initial peak PA intensity scales linearly with the pump fluence; thus, the excitation densities are well below the absorption saturation threshold. At low excitation densities, the magnitude after 100 ps also scales linearly, a confirmation that at these low excitation densities, the intensity dependent decay does not compete with the natural lifetime of the exciton. Above pump fluences of $\sim 1 \mu\text{J cm}^{-2}$ (an excitation density of 1.5

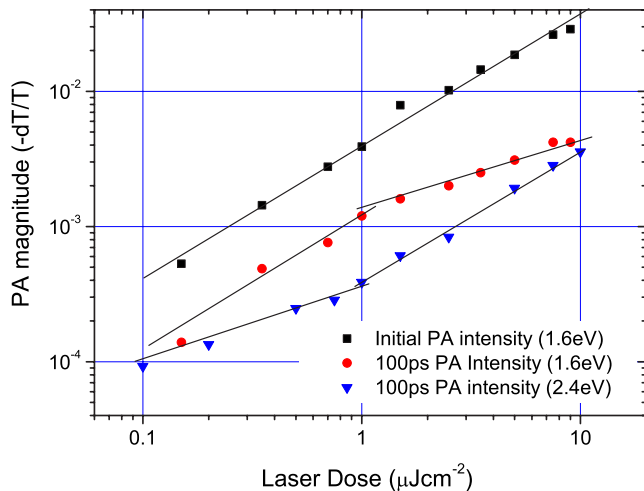


FIG. 3. (Color online) Excitation dose dependences for the intensity of the PA absorption at 1.6 and 2.4 eV. Straight lines of gradient 0.5 and 1 are drawn as a guide to the eyes.

$\times 10^{17} \text{ cm}^{-3}$), a deviation from the linear relationship is observed; in a double logarithmic presentation, the relationship turns over to a slope of approximately 0.5. It is also important to note that at a similar threshold, the intensity of the PA at 2.4 eV, the charged state absorption (including a small contribution from the overlap of the singlet features), also shows an additional increase in intensity.

The change of the singlet excitation density dependence (after 100 ps) to a slope of ~ 0.5 at high excitation densities is the result of a bimolecular exciton quenching process, dominating the decay above a threshold pump fluence of $\sim 1 \mu\text{J cm}^{-2}$ (2×10^{12} photons cm^{-2}). The only feasible scenario for a bimolecular reaction in a pristine film is that of the singlet-singlet annihilation (SSA).²² The charges that are formed by this reaction are responsible for the characteristic charge state absorption at 2.4 eV. This threshold pump fluence for SSA, which is smaller than some previously reported values for conjugated polymers,¹¹ is measured directly without the need to fit data to complex models of exciton dynamics which are often necessary when data are only available at higher excitation densities.^{11,22,27,28} This could, in part, explain the apparent confusion over the mechanism of charge generation in ultrafast experiments in conjugated polymers.

The bimolecular annihilation reaction can proceed via two mechanisms; the rate limiting step could be either the energy transfer itself as would be expected from a purely long range Förster mechanism. Alternatively, the diffusion of the excitons between neighboring chains can give rise to an additional interaction either by a collisional- or Dexter-type electron transfer process or by migration into the Förster-radius of another exciton again yielding Förster-type energy transfer. Both mechanisms lead to the generalized rate equation,

$$\frac{dN}{dt} = G(t) - \frac{N}{\tau} - \gamma(t)N^2, \quad (1)$$

where $G(t)$ represents the exciton generation function, N is the exciton density, τ is the exciton lifetime, and $\gamma(y)$ the

annihilation parameter, which can, in some cases, have a time dependence.

The condition for energy transfer by the long range Förster interaction is that there must be an overlap of the fluorescence of the donor and the absorption of the acceptor (the excited singlet state). From which it is possible to calculate the Förster radius, i.e., the separation required for energy transfer to compete with the unquenched decay of the singlet, this parameter is defined by Förster's equation,

$$R_0^6 = \frac{9000(\ln 10)\kappa^2 Q_D}{128\pi^5 N n^4} \int F_D(\lambda) \epsilon_A(\lambda) \lambda^4 d\lambda, \quad (2)$$

where Q_D is the fluorescence quantum yield in the absence of the acceptor, n is the refractive index of the medium, N is Avogadro's number, and κ^2 is the factor describing the relative orientation of the donor and acceptor dipoles, normally assumed to be equal to $2/3$. $F_D(\lambda)$ is the normalized fluorescence of the donor and $\epsilon_A(\lambda)$ is the absorption spectrum of the acceptor. Given the small overlap between the singlet fluorescence of PF2/6 and its photoinduced absorption spectrum, we find that this calculated Förster radius, $R_{SSA} = 11 \pm 5 \text{ \AA}$, is of the same magnitude to the typical separation of the polymer chains in the film.²⁹ For the rapid quenching observed due to SSA, the typical separation of the excitons would be required to be considerably smaller than this, implying intrachain singlets. However, SSA is observed for relatively low excitation densities, for example, an excitation dose of $6 \mu\text{J cm}^{-2}$ gives a mean separation of the excitations of approximately 10 nm. Hence, for the simplistic case of static quenching by the long range dipole interaction, annihilation would not be expected to take place. Referring once again to Fig. 2, it is clear that at low temperature, for comparable pump fluences, the effect of annihilation is appreciably less. The thermal activation of the annihilation gives an indication of the cause of the lower than expected threshold: exciton diffusion. Previous studies of the effect of temperature on the quenching rate of simple polymer-dopant systems³⁰ have shown that the rate of diffusion of singlet excitons in polyfluorene changes from $0.43 \text{ nm}^2 \text{ ps}^{-1}$ at 10 K to $1.44 \text{ nm}^2 \text{ ps}^{-1}$ at 300 K. In the SSA case, excitons are able to move faster and further at high temperature and the effect of annihilation is greater. An additional factor which could further increase the distances that the excitons interact over is the spatial extent of the exciton itself, which in some cases extends over approximately 5 nm, limiting the usefulness of the point dipole approximation.³¹ The very short Förster radius, which is comparable to the size of the exciton, would suggest that the energy transfer is a Dexter-type exchange interaction as this would be expected to dominate at the length scales where there is overlap of the donor and acceptor orbitals.³²

Fitting the data to the integrated rate equation becomes complicated by the possibility of the quadratic annihilation term in Eq. (1) having a time dependent coefficient $\gamma(t)$. In order to fit the data, we use a modification of the method of Dogariu *et al.*¹⁰ With this method, the calculation of the time dependence of the SSA coefficient is made by renormalizing the data with a new variable,

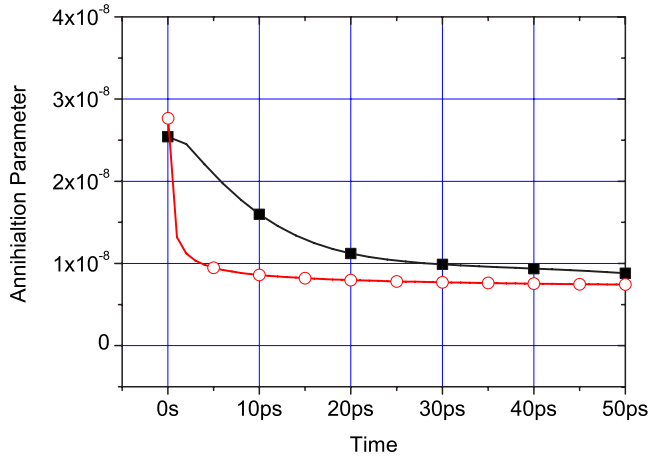


FIG. 4. (Color online) Time dependence of the singlet-singlet annihilation parameter γ at 10 K. The curves are calculated from the transient absorption data (filled squares) and a theoretical plot of the expected annihilation parameter from Eq. (4), using the values of R and D given in the text (hollow circles).

$$y(t) = e^{-t/\tau}N(t), \quad (3)$$

where $N(t)$ is the singlet population when SSA is active and τ is the lifetime of the singlet when there is no annihilation. It then follows that the rate equation becomes

$$\frac{dy}{dt} = \gamma(t)e^{-t/\tau}. \quad (4)$$

From Eq. (4) it is possible to extract the annihilation parameter, with full time dependence, $\gamma(t)$, from the data by calculating the derivative of the function $y(t)$. Previously, this had proved difficult due to the noise on the data and an integral form of $\gamma(t)$ was derived. However, by fitting our data with a multiexponential model to accurately reproduce the shape of the curve and using this as $N(t)$ it is possible to directly plot $\gamma(t)$ (Fig. 4). The initial annihilation parameter is $\gamma(0) = 2.5 \times 10^{-8} \text{ cm}^3 \text{ s}^{-1}$ at 10 K and $\gamma(0) = 9.5 \times 10^{-8} \text{ cm}^3 \text{ s}^{-1}$ at 300 K.

The calculated annihilation parameter is not constant over time; in molecular crystals, the same behavior has previously been observed.²¹ In this case, the annihilation parameter decreases with time because the diffusion constant is small compared to the spatial distribution of the states; as a result, there is a localized depletion of the exciton density which is not compensated for by diffusion. This leads to the time dependence of the annihilation parameter of the form:^{10,33}

$$\gamma(t) = 4\pi DR \left(1 + \frac{R}{\sqrt{\pi Dt}} \right), \quad (5)$$

where D is the diffusion constant and R the radius of the interaction. However, after the first few picoseconds, our system is in the high diffusion regime, i.e., $D > R^2/\pi t$, so the equation can be simplified to $\gamma = 4\pi DR$, which no longer contains any intrinsic time dependence. Figure 4 shows the calculated time dependence of $\gamma(t)$ from the experimental data at 10 K compared to the expected time dependence

from Eq. (3). The shape of the time dependence of the theoretical and the experimental curves is different since γ remains higher for longer than would be expected from the model. The higher annihilation rate in the intermediate time is due to the nature of energy transfer in conjugated polymers. The large inhomogeneous broadening of the spectrum of CPs leads to a time dependence of the diffusion constant. The exciton diffusion is enhanced in the early time by downhill migration to lower energy chain segments and then once the excitons are thermalized, slower diffusion takes over.^{34,35} This time dependence of the exciton diffusion contributes to the observed time dependence of $\gamma(t)$, keeping the annihilation rate higher for longer while the excitons are able to move faster due to the dispersive component in the migration. At longer times after the dispersive migration is over, the annihilation rate tends toward the theoretical constant value given by Eq. (5).

SINGLET-TRIPLET ANNIHILATION

In a similar way to SSA, it is possible for singlet excitons to be quenched by triplet excitons. Once again, the Förster radius for the interaction can be calculated from the overlap of the singlet fluorescence and the widely reported triplet excited state absorption for polyfluorene.³⁶ This is larger than for the singlet-singlet interaction, $R_{\text{STA}} = 21 \pm 5 \text{ \AA}$. For the simple case of Förster transfer, it implies that it should be comparatively easier for the singlets to annihilate with triplets than with other singlets. By allowing a background of triplets to build up using a cw laser with the sample at low temperature and then measuring the singlet lifetime, it is possible to see the effect of singlet-triplet annihilation on the singlet population.

Evaluation of the effect of the background triplet population on the singlet kinetics requires knowledge of the triplet population in the film. Estimation of the triplet population is not a trivial process given that even for low temperatures, high excitation densities cause triplet-triplet annihilation to dominate the decay of the triplets. This leads to a quadratic term in the rate equation for cw excitation,

$$\frac{dN_T}{dt} = A - \gamma_{TT}N_T^2 - k_rN_T. \quad (4')$$

Considering that the rate of radiative decay is very slow compared to the rate that the excitons annihilate, the phosphorescence term can be effectively ignored. This gives a solution for Eq. (4'), where the steady-state triplet density is proportional to $\sqrt{A/\gamma_{TT}}$ (where A is the rate of triplet generation and γ_{TT} the triplet-triplet annihilation parameter). A more detailed description of the modeling of the triplet population is given in our previous work.³⁷ The precise determination of γ_{TT} in the solid state has been previously made for a number of polyfluorenes and polyfluorene derivatives. A large spread of values is reported for the triplet-triplet annihilation parameter of conjugated polymers at low temperature with results between 10^{-15} and 10^{-13} s^{-1} published.^{37,38} From the calculated cw triplet excitation density, it is possible to work back to the separation of the triplet and singlet

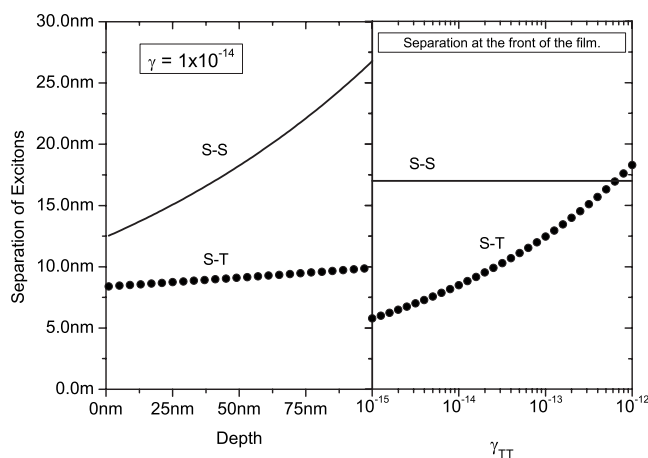


FIG. 5. Variation of the separation of singlet excitons at the point where SSA dominates the decay of the singlet excitons (solid) and singlet-triplet separation when a background of triplet is created with cw excitation (dots). Variation with depth into the sample (left) and triplet-triplet annihilation rate (right).

states during the experiment. Based on the assumption that the maximum separation of a singlet and a triplet occurs when the singlet exciton is placed halfway between two triplets, the variation of the singlet to triplet distance with γ_{TT} is shown on the right hand panel of Fig. 5. Also shown, for comparison, is the mean separation of singlets at the threshold for SSA. For the singlet-triplet separation to become greater than the singlet-singlet separation at the threshold for SSA, the TTA rate would have to be approximately ten times the highest reported values. The left panel of Fig. 5 shows the variation of singlet separation and the variation of the singlet-triplet (S-T) separation with depth into the sample, calculated using the Beer-Lambert law for the singlet distribution and the Beer-Lambert law in combination with the above equation for the S-T distance. Both the calculations in Fig. 4 show that the S-T distance during cw photoexcitation is always less than the singlet separation required for SSA. The number of triplets created by the femtosecond pump beam can effectively be ignored as the cw power of the femtosecond beam during the experiments was less than 1 mW cm^{-2} , negligible compared to the cw excitation beam used to generate a background of triplets. In order to prevent the confusing effect of observing both SSA and STA, the femtosecond excitation beam was kept below the threshold for SSA during the experiment.

It was found that measurement of the singlet lifetime with a background triplet population at low temperature has no effect on the decay rate of the singlet excitons. Figure 6 shows a comparison between the decay of the singlet photoinduced absorption signal for a thin film of PF2/6 both with and without a background triplet population; the decay remains unchanged throughout the whole of the singlet lifetime. Although unexpected, this result is in agreement with our previous work showing that the cw photoluminescence and electroluminescence intensity are additive. When a device is simultaneously excited optically and electrically, the emission intensity is the same as the sum of the fluorescence from the individual electrical and optical excitations.³⁹ Both

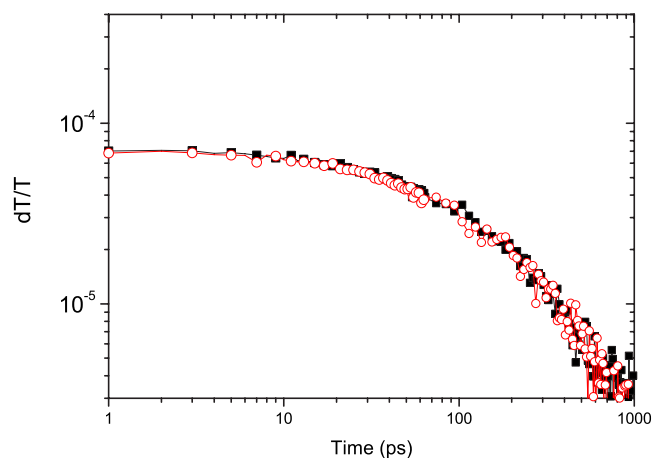


FIG. 6. (Color online) Decay of the singlet exciton PA feature both with (○) and without (■) a background of triplet population, for cw excitation (100 mW cm^{-2}).

these measurements show that the large background of triplets created in a polymer either optically or electrically does not significantly quench the singlets. The implications of this are very promising especially for the potential maximum efficiency of PLEDs running at high brightness.

In the first instance, it seems unremarkable that STA is not observed, as the separation between singlets and triplets is greater than the Förster radius of the interaction. What is surprising is that the singlet-singlet annihilation, for similar Förster radius and separation of excitons, is very efficient due to the diffusion of excitons; thus the SSA is strongly activated by diffusion and STA is not. To understand the process that causes this, we return to the earlier observation on the mechanism of the energy transfer. At the short distances that are involved in SSA, Dexter transfer dominates the annihilation process. Therefore, we can assume that both the SSA and STA proceed via a Dexter-type electron exchange mechanism. One of the requirements for Dexter transfer is an overlap of the electronic orbitals of the donor and the acceptor. For SSA where the singlet orbitals involved are identical and spatially large, this is easy to achieve. However, the overlap between singlet and triplet orbitals is less. This is partially due to the differing shape of the singlet and triplet states. The singlet states are oriented parallel to the chain, whereas the triplet states are oriented perpendicular to the chain; thus, the overlap of the states necessary for electron exchange is difficult due to symmetry constraints.⁴⁰ Also the differing spatial extent of the states becomes important. If it is assumed that the polymer chain is divided into segments bound by conformational or chemical defects, one normally assumes that the singlet exciton occupies most of the segment, a phenomenon known as the effective conjugation length (typically 25–30 repeat units).^{41,42} Conversely, the triplet exciton is understood to only occupy a segment of a few phenyl rings;^{43–45} thus, if the reasonable assumption that each chain segment can only hold one excitation (either singlet or triplet), then the mean distance from the singlet to the neighboring triplet exciton is large and the necessary overlap of the states required for intrachain STA by Dexter transfer would not be possible. Additionally, given this constraint, the

singlet would be outside the Förster radius of the triplet and the energy transfer could not proceed by a Förster mechanism either.

CONCLUSION

Singlet-singlet annihilation has been observed to become the dominant decay mechanism for singlets even for a low pump threshold of $\sim 1 \mu\text{J cm}^{-2}$, corresponding to an excitation density of $1.5 \times 10^{17} \text{ cm}^{-3}$. The process is entirely diffusion controlled and a time dependence of the annihilation parameter is observed due to the inherent time dependence of diffusion controlled process as well as the effect of dispersive migration on the diffusion rate in the initial time. The

low pump fluence required for SSA highlights the importance of using low excitation densities in ultrafast studies of conjugated polymers and could be the cause of some of the confusion over the nature of charge generation by photoexcitation. Additionally, we find no evidence of the singlet-triplet annihilation when there is a background triplet density comparable to the singlet density required for SSA; this is attributed to the differing shape and spatial extent of the singlet and triplet states involved.

ACKNOWLEDGMENTS

We acknowledge support from CENAMPS and One North East and S.M.K. thanks the Durham Photonic Materials Institute.

-
- ¹J. H. Burroughes, D. D. C. Bradley, A. R. Brown, R. N. Marks, K. Mackay, R. H. Friend, P. L. Burns, and A. B. Holmes, *Nature (London)* **347**, 539 (1990).
- ²Y. Ohmori, M. Uchida, K. Muro, and K. Yoshino, *Jpn. J. Appl. Phys., Part 2* **30**, L1941 (1991).
- ³M. N. Shkunov, R. Osterbacka, A. Fujii, K. Yoshino, and Z. V. Vardeny, *Appl. Phys. Lett.* **74**, 1648 (1999).
- ⁴N. Tessler, N. T. Harrison, and R. H. Friend, *Adv. Mater. (Weinheim, Ger.)* **10**, 64 (1998).
- ⁵N. Tessler, G. J. Denton, and R. H. Friend, *Nature (London)* **382**, 695 (1996).
- ⁶M. Yan, L. J. Rothberg, F. Papadimitrakopoulos, M. E. Galvin, and T. M. Miller, *Phys. Rev. Lett.* **73**, 744 (1994).
- ⁷V. I. Arkhipov, E. V. Emelianova, and H. Bassler, *Phys. Rev. B* **70**, 205205 (2004).
- ⁸D. Neher, *Macromol. Rapid Commun.* **22**, 1366 (2001).
- ⁹G. Lanzani, G. Cerullo, D. Polli, A. Gambetta, M. Zavelani-Rossi, and C. Gadermaier, *Phys. Status Solidi A* **201**, 1116 (2004).
- ¹⁰A. Dogariu, D. Vacar, and A. J. Heeger, *Phys. Rev. B* **58**, 10218 (1998).
- ¹¹E. S. Maniloff, V. I. Klimov, and D. W. McBranch, *Phys. Rev. B* **56**, 1876 (1997).
- ¹²C. Silva, A. S. Dhoot, D. M. Russell, M. A. Stevens, A. C. Arias, J. D. MacKenzie, N. C. Greenham, R. H. Friend, S. Setayesh, and K. Mullen, *Phys. Rev. B* **64**, 125211 (2001).
- ¹³C. Gadermaier, G. Cerullo, G. Sansone, G. Leising, U. Scherf, and G. Lanzani, *Phys. Rev. Lett.* **89**, 117402 (2002).
- ¹⁴V. I. Arkhipov, E. V. Emelianova, and H. Bassler, *Chem. Phys. Lett.* **340**, 517 (2001).
- ¹⁵R. Kersting, U. Lemmer, M. Deussen, H. J. Bakker, R. F. Mahrt, H. Kurz, V. I. Arkhipov, H. Bassler, and E. O. Gobel, *Phys. Rev. Lett.* **73**, 1440 (1994).
- ¹⁶E. Frankevich, H. Ishii, Y. Hamanaka, T. Yokoyama, A. Fuji, S. Li, K. Yoskino, A. Nakamura, and K. Seki, *Phys. Rev. B* **62**, 2505 (2000).
- ¹⁷I. B. Martini, A. D. Smith, and B. J. Schwartz, *Phys. Rev. B* **69**, 035204 (2004).
- ¹⁸B. Kraabel and D. W. McBranch, *Chem. Phys. Lett.* **330**, 403 (2000).
- ¹⁹C. Daniel, L. M. Herz, C. Silva, F. J. M. Hoeben, P. Jonkheijm, A. Schenning, and E. W. Meijer, *Phys. Rev. B* **68**, 235212 (2003).
- ²⁰T. Virgili, D. Marinotto, C. Manzoni, G. Cerullo, and G. Lanzani, *Phys. Rev. Lett.* **94**, 117402 (2005).
- ²¹M. Pope and C. E. Swenberg, *Electronic Processes in Organic Crystals and Polymers* (Oxford University Press, Oxford, 1999).
- ²²Q. H. Xu, D. Moses, and A. J. Heeger, *Phys. Rev. B* **68**, 174303 (2003).
- ²³B. Kraabel, V. I. Klimov, R. Kohlman, S. Xu, H. L. Wang, and D. W. McBranch, *Phys. Rev. B* **61**, 8501 (2000).
- ²⁴D. W. McBranch, B. Kraabel, S. Xu, R. S. Kohlman, V. I. Klimov, D. D. C. Bradley, B. R. Hsieh, and M. Rubner, *Synth. Met.* **101**, 291 (1999).
- ²⁵H. D. Burrows, J. S. de Melo, M. Forster, R. Guntner, U. Scherf, A. P. Monkman, and S. Navaratnam, *Chem. Phys. Lett.* **385**, 105 (2004).
- ²⁶C. Y. Chi, C. Im, and G. Wegner, *J. Chem. Phys.* **124**, 024907 (2006).
- ²⁷C. Silva, M. A. Stevens, D. M. Russell, S. Setayesh, K. Mullen, and R. H. Friend, *Synth. Met.* **116**, 9 (2001).
- ²⁸C. Silva, D. M. Russell, M. A. Stevens, J. D. Mackenzie, S. Setayesh, K. Mullen, and R. H. Friend, *Chem. Phys. Lett.* **319**, 494 (2000).
- ²⁹M. Knaapila, K. Kisko, B. P. Lyons, R. Stepanyan, J. P. Foreman, O. H. Seeck, U. Vainio, L. O. Palsson, R. Serimaa, M. Torkkeli, and A. P. Monkman, *J. Phys. Chem. B* **108**, 10711 (2004).
- ³⁰B. P. Lyons and A. P. Monkman, *Phys. Rev. B* **71**, 235201 (2005).
- ³¹H. Wiesenhofer, D. Beljonne, G. D. Scholes, E. Hennebicq, J. L. Bredas, and E. Zojer, *Adv. Funct. Mater.* **15**, 155 (2005).
- ³²J. R. Lakowicz, *Principles of Fluorescence Spectroscopy* (Kluwer Academic, New York, 1999).
- ³³R. C. Powell and Z. G. Soos, *J. Lumin.* **11**, 1 (1975).
- ³⁴S. C. J. Meskers, J. Hubner, M. Oestreich, and H. Bassler, *J. Phys. Chem. B* **105**, 9139 (2001).
- ³⁵K. Brunner, J. van Haare, B. M. W. Langeveld-Voss, H. F. M. Schoo, J. W. Hofstraat, and A. van Dijken, *J. Phys. Chem. B* **106**, 6834 (2002).
- ³⁶C. Rothe, S. M. King, F. Dias, and A. P. Monkman, *Phys. Rev. B* **70**, 195203 (2004).

- ³⁷C. Rothe, H. A. Al Attar, and A. P. Monkman, Phys. Rev. B **72**, 155330 (2005).
- ³⁸M. Westerling, C. Vijila, R. Osterbacka, and H. Stubb, Phys. Rev. B **69**, 245201 (2004).
- ³⁹C. Rothe, S. M. King, and A. P. Monkman, Phys. Rev. Lett. **97**, 076602 (2006).
- ⁴⁰S. M. King, H. L. Vaughan, and A. P. Monkman, Chem. Phys. Lett. **440**, 98 (2007).
- ⁴¹K. Mullen and G. Wegner, *Electronic Materials: The Oligomer Approach* (Wiley-VCH, Weinheim, 1998).
- ⁴²J. Rissler, Chem. Phys. Lett. **395**, 92 (2004).
- ⁴³A. van Dijken, J. Bastiaansen, N. M. M. Kiggen, B. M. W. Langeveld, C. Rothe, A. Monkman, I. Bach, P. Stossel, and K. Brunner, J. Am. Chem. Soc. **126**, 7718 (2004).
- ⁴⁴L. S. Swanson, J. Shinar, and K. Yoshino, Phys. Rev. Lett. **65**, 1140 (1990).
- ⁴⁵E. J. W. List, J. Partee, J. Shinar, U. Scherf, K. Mullen, E. Zojer, K. Petritsch, G. Leising, and W. Graupner, Phys. Rev. B **61**, 10807 (2000).